Peristerite - the Billion-Year-Old Mirror

Ralph S Conti PhD

Figure 1. Peristerites from McDonald mine Hybla, Ont. Collected ~1965. Large one dubbed the "Arkenstone" is a 22.5cm crystal, while the smaller is a 3 cm crystal with a doubly-terminated smokey quartz.

Peristerite is a rock type consisting of an intergrowth of two types of plagioclase feldspars, albite and oligoclase. When the intergrowth is highly ordered at dimensions comparable to the wavelength of visible light, a colorful schiller (labradorescence - Figure 1 and Figure 2) can occur. This arises from constructive interference from multiple interfaces between the two feldspars. Very special conditions must occur to form these precise and beautiful structures; these conditions were to be found circa one billion years ago deep in the roots of a Himalaya-sized Mountain range. Here we explore what these structures are, how they cause light to interfere, and why the conditions were right for their formation in the Grenville Orogeny, during assembly of the supercontinent Rodinia.

Figure 2. Peristerite cabochon (11cm) from Quadeville, Ont. collected in the 1960s.

Bragg Mirrors – the optical elements creating labradorescence

Multi-layer dielectric (as opposed to metallic) coatings or Bragg mirrors are inarguably indispensable to all modern laser optics, such as in Figure 3. The first man-made invention of multi-layer dielectric coatings to create a Bragg mirror was by Walter Geffcken at the Schott Glass company [Geffcken 1939]. Biological evolution has produced such structures for hundreds of million years in a wide variety of species (see Figure 4 [Moreau 2020]), including birds, moths, beetles, etc. Geochemistry, however, predates both these mechanisms, epitomized by the one-billion-year-old mirrors shown here. While the man-made and biological products of multi-layer dielectrics are engineered or evolved to create a great variety of transmission and reflection effects (hot-mirrors, cold mirrors, broad-band mirrors, interference filters, anti-reflection coatings, colorful displays, camouflage, laser-line-blocking glasses, single-wavelength mirrors), geological serendipity in feldspars predominantly produces only the simplest layering schemes. To produce colors, the requirements on layer spacings, transparency, and alignment are fulfilled only under special formation and reprocessing environments.

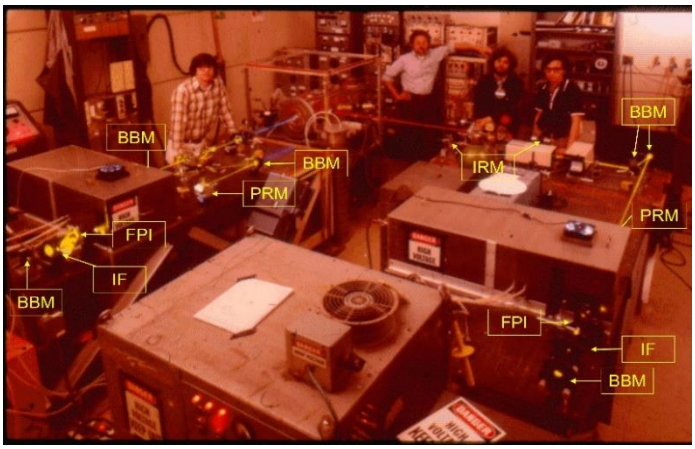

Figure 3. Multi-layer dielectric optical elements for 1979 Parity Non-Conservation Experiment. Broad-Band Mirrors (BBM) are 99% reflective across the visible spectrum and used here to direct the beams from two tunable dye lasers. In addition, they serve as end mirrors for each laser optical cavity. Partially reflective (50%) Broad-Band mirrors (PRM) provide the laser output. Interference Filters (IF) and Fabry-Perot Interferometers (FP) are intra-cavity laser tuning elements. Infrared Mirrors (IRM) steer a down-stream infrared beam. All these multi-layer dielectric elements are engineered to exhibit desired reflection and transmission properties with minimal absorption. Photo LBL.

Figure 5 details how the Bragg Mirror effect, labradorescence, is produced by regularly spaced, alternating parallel planes of two different feldspars

(albite and oligoclase in peristerite) with differing indices of refraction ($\frac{\lambda_{norm}}{2} = \frac{d_1}{n_1} + \frac{d_2}{n_2}$). The reflections occur in only one mirrored direction, with their local color tuning only weakly with the light incidence angle. If the sample is sufficiently transparent the transmitted light lacks the reflected color. This behavior is characteristic and can be distinguished from opalescence, which is a diffraction effect (Figure 6) that sprays different colors in different directions for the same incidence angle. For normal incidence, the interface between two dielectric materials (albite and oligoclase) will reflect a portion of the light according to $A = \frac{n_a - n_o}{n_a + n_o}$, where $R = |A|^2$ is the reflected fraction and n_a and n_o are the respective indices of refraction [Fresnel]. Each interface may only give small reflection, yet, if m reflections are coherent (interfere constructively *i.e.,* maintain constant $\frac{\lambda_{norm}}{2}$ bilayer thickness) one can get large total reflectivity $R = |m * A|^2$ for the effective wavelength in the medium, λ_{norm}.

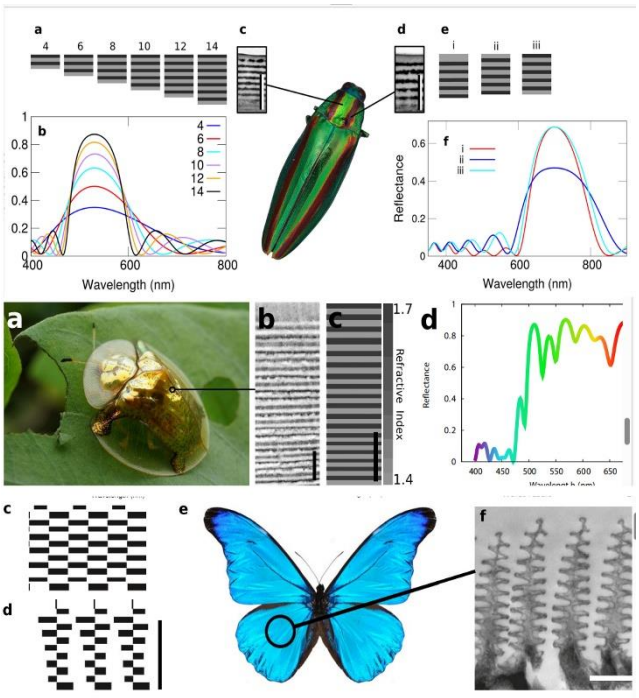

Figure 4 In [Moreau 2020] the authors make computer models that try to mimic the structures evolved in beetles and butterflies, using both multi-layer dielectric and diffractive effects. They aim to engineer novel biologically-inspired optics.

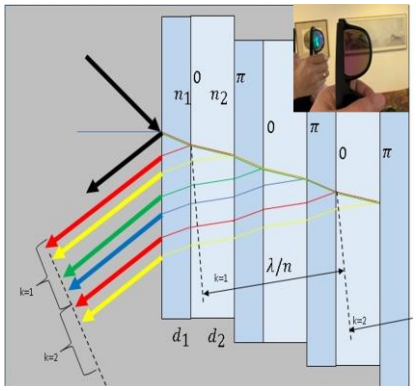

Figure 5. Principles of the multi-layer Dielectric Mirror or Bragg Mirror. A one-color, high-reflectance mirror can be formed by multiple alternating layers of material with differing indices of refraction ($n_1 < n_2$). Light will be reflected at each interface with amplitude $A = \frac{n_1 - n_2}{n_1 + n_2}$ (phase shift 0 for going from lower index to higher and π for high to low). For normal incidence, light with $\frac{\lambda_{norm}}{2} = \frac{d_1}{n_1} + \frac{d_2}{n_2} \cong \frac{d_1 + d_2}{n}$ ($n \equiv \frac{n_1 + n_2}{2}$) will be constructively reflected at all interfaces. To clarify the interference of various reflections, the diagram shows non-normal incidence. The different path colors only label different path types (red and green for 0 phase shift paths and yellow and blue for π). The reflected color tunes only weakly with incidence angle ($\frac{\sin\theta_{out}}{1} = \frac{\sin\theta_{in}}{n}$, $\lambda = \lambda_{norm} \cos\theta_{in}$. This is illustrated in the upper right inset: sunglasses with a multi-layer dielectric coating on the front are held facing a large mirror. At near normal incidence they reflect green, while more glancing angles reflect blue. In transmission, the image of the wall reflected in the big mirror acquires a rosy hue due to removal of the green (example of an interference filter).

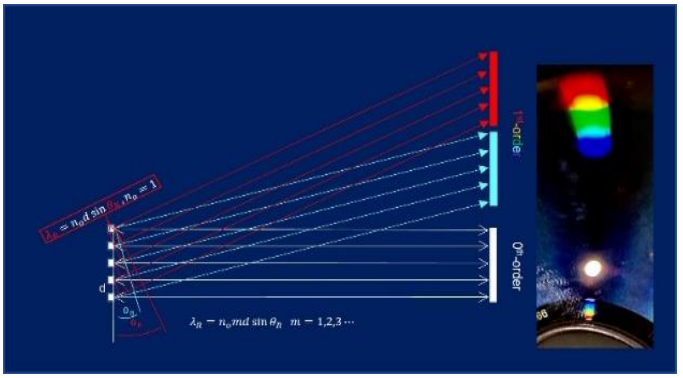

Figure 6. Diffraction Grating principles. Incident white light strikes a grating of spacing d. First-order colors are diffracted such that they are angled to acquire one extra wavelength relative to adjacent grating reflectors. Thus each wavelength is diffracted at its own particular angle. In 0-order reflection, all colors are in phase and specularly reflected. Insert to the right, shows diffraction from a DVD. The spectrum is not continuous, due to the discrete colored LEDs used in the illuminating iPhone flashlight.

Peristerite

Mindat [MindatPeri] describes peristerite as: “A variety of albite showing slight iridescence and sometimes adularescence (as in moonstone)”. The “iridescence” (more properly labradorescence, labradorization, schiller, or even peristerescence) is hardly slight in Figure 1 and Figure 2, as are in many entries in the Mindat photo gallery (46 total entries, 34 clearly showing labradorescence colors, 20 of which are from the Bancroft Terrane).

Figure 7 Adularescent peristerite from the CN Dump in Bancroft Ont. The bright spot on the cabochon surface is a ghostly glow that moves with lighting angle (opposite to surface specular reflection). The bilayers here are thicker than in labradorescent samples and result in multiple reflective peaks across the visible spectrum (see image to the right and the accompanying discussion in the text). This can be called a “moonstone” since it exhibits the same properties and operates on the same optical principles as the more usual adularia moonstones.

Adularescence is now also being considered as a Bragg mirror phenomenon. According to the International Gem Society [IGS 2023], “If the albite plates are thick, the sheen is white”. Figure 7 shows a rough cabochon of adularescent peristerite from the Golding-Keene Mine (via the CN dump, Bancroft [CN Dump 2023]). The point of the image to the right (a rotated version of one in Figure 6) is to show that the “white” light produced by the iPhone flashlight can be reproduced by the multiple peaks of a Bragg mirror with thick bilayers; if yellow has a calculated peak resonance for 10 half-wavelengths, then 9 to 13 should reproduce an adularescence that is as white to the eye as the iPhone flashlight.

An electron-microscope study of peristerite plagioclases

By S. G. Fleet

Department of Mineralogy and Petrology, University of Cambridge

and

P. H. Ribbe

Crystallographic Laboratory, Cavendish Laboratory, University of Cambridge, and Department of the Geophysical Sciences, University of Chicago

[Read 28 May 1964]

Table I. Particulars of the peristerites studied

No.	Specimen locality	Composition (wt. %)* An	Or	Nature of schiller†	Nature of unmixing
1	Auburn, Maine	2·8*	0·4	Pale blue, medium to weak	Infrequent lamellae, alt. thick & thin
2	Hybla, Ontario	7·0	1·0	Yellow to blue, very strong	Infrequent lamellae, alt. thick & thin
3	Monteagle Township, Ontario	7·6	1·0	Pale blue, strong	Infrequent lamellae, alt. thick & thin
4	Bancroft, Ontario	8·3	0·5	Blue, strong	Infrequent lamellae, alt. thick & thin
5	Haddam, Connecticut	8·8	0·5	Pale blue, weak	Frequent lamellae
6	Villeneuve, Quebec	10·3	0·7	Pale blue, medium	Infrequent lamellae, alt. thick & thin
7	Froland, Norway	10·5	1·2	Blue to white, very strong	Frequent lamellae
8	Peekskill, New York	11·7	0·6	None visible (small grains)	Frequent lamellae
9	Monteagle Valley, Ontario	12·4	1·0	None visible	Infrequent lamellae
10	Bakersville, North Carolina	17·0	3·1	None visible	No lamellae

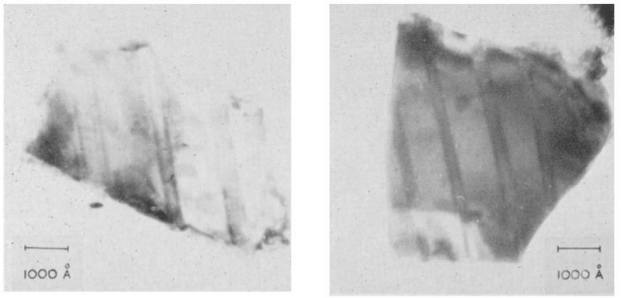

Fig. 5. Bright-field micrographs of typical grains of: (i), left, Hybla peristerite (7·0 % An); (ii), right, Monteagle Township peristerite (7·6 % An).

Figure 8. Selected images from [Ribbe 1964] showing uniformly-spaced, parallel alternating plates of albite (thick) and oligoclase (thin) with optical half-wavelenth dimensions

Peristerite Structure

In 1924 Ove BØggild published a paper [Bøggild 1924] (see also the Appendix) on his investigation of what he coined as *labradorization* and is now called *labradorescence*. He systematically determined the orientation of the Bragg mirror planes for the great variety of feldspars (peristerite, labradorite, microcline, larvikite, and orthoclase). The focus here is optical peristerite structure and how this delicately fine-tuned assemblage can occur naturally. The definitive work on peristerite was done by Fleet and Ribbe [Ribbe 1964] as summarized in Figure 8. They employed transmission electron microscopy and electron diffraction methods on ten peristerites from around the world to characterize

the exosolution of the peristerite solid-solution into its albite and oligoclase low-temperature components. They saw the repeating bi-layer structure that matches the Bragg mirror scenario of Figure 5, with a 13° inclination to (010), corresponding to the $(0\bar{8}1)$ plane (Bøggild had this orientation as well). A conceptual view of how the two feldspars might separate into a lower energy state is shown in Figure 9.

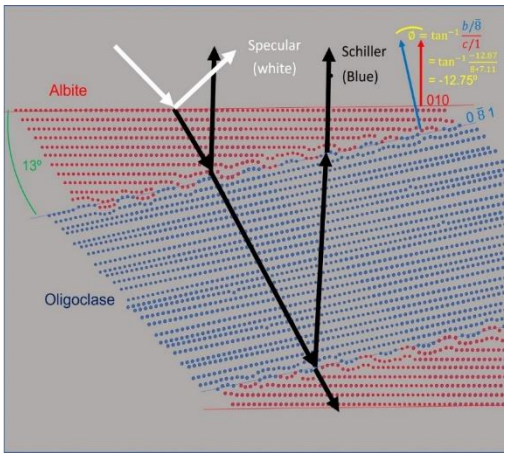

Figure 9. Conceptual view of how a lower energy state might be attained through unmixing across the $0\bar{8}1$ interface. Red and blue dots represent albite and oligoclase unit cells, respectively.

Ribbe's sample number 2 in Figure 8 from Hybla Ont., (same locale as Figure 1) showed very strong yellow to blue schiller (=labradorization = labradorescence) with a maximum albite thickness of 170nm. To get yellow labradorescence from this sample, would require a bi-layer thickness of $d = \frac{\lambda}{2n} = \frac{590\text{ nm}}{2*1.53} = 193\text{ nm}$ (e.g. 160 nm albite, 33 nm oligoclase). Local patches (1-5 mm) in Figure 1 and Figure 2 exhibit all the colors of the visible spectrum and Ribbe's results show that ½ wavelength Bragg mirrors match the required characterization perfectly. One final reality check: Are these peristerites transparent enough and uniformly spaced enough to allow the labradorescence to dominate over surface specular reflection ($R_{spec} = |A_{spec}|^2 = \left|\frac{n_a - n_{air}}{n_a + n_{air}}\right|^2 = \left|\frac{1.53-1}{1.53+1}\right|^2 = 0.044$)? It is difficult to know what the precise indices of refraction of albite and oligoclase are along the mirror axis, however an order-of-magnitude guess for a single interface is $R_{peri} = |mA_{peri}|^2 = \left|m\frac{n_a - n_o}{n_a + n_o}\right|^2 = \left|m\frac{1.534-1.544}{1.534+1.544}\right|^2 = |-0.0032m|^2 = m^2 1.0 \times 10^{-5}$. Of course, the amplitude cannot exceed 1, but it should be near that in order to dominate the specular reflection, thus requiring at least 300 coherent bilayers. Since the bi-layer thickness is being matched to a half wavelength in the medium, it can vary up to 20% without seriously affecting the coherence, merely broadening the reflected frequencies at the cost of a factor of 2 or 3 in the number of bi-layers. Figure 10 shows the sample of Figure 2 with lighting oriented in a geometry that shows the labradorescence for the two albite twin (see Figure 11) directions (the top picture viewed the stone rotated by 180° and the image was rotated back). The ellipses show where the ~1mm twin planes intersect the cabochon surface. Notice that the fields of labradorescence for the twins overlap. In particular, the center of the top picture is thick enough (0.5 to 0.3mm) to show labradorescence without seriously attenuating that from the twin beneath in the lower picture. Thus, there is enough transparency for $m = \frac{0.3\text{ mm}}{193\text{ nm}} = 1500$, well above that required.[1]

Figure 10. Labradorescence from twin planes of cabochon from Figure 2 Top image was taken with the same lighting as the bottom image with the cab physically rotated by 180° and then the image is rotated back.

[1] Note in Figure 5 the interfaces with 0 and π phase shift are treated separately. If they have equal thickness they will add coherently giving another factor of 4 in the reflection. According to Ribbe the albite is 3 to 4 times the

Feldspar Geochemistry

Feldspars are aluminum tecto-silicates forming two solid-solution series, between albite and orthoclase (alkali feldspars) and between albite and anorthite (plagioclase), as shown in Figure 12. They form orthorhombic crystals (orthoclase, sanidine) or triclinic crystals (anorthite, bytownite, labradorite, andesine, oligoclase, albite, anorthoclase, and microcline) with angles near to those for orthorhombic orthoclase.

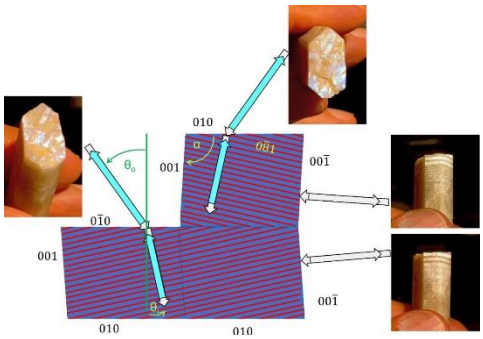

Figure 11 albite twinning, labradorescence. Albite twinning consists of a reflection through the (010) plane. Since angle α is 93.45°, back reflections from the two $(00\bar{1})$ twin planes are separated by 6.9°. The labradorescence angle ϑ_i=13° -> ϑ_o=20° is reversed in the twin. Stills from a video under different viewing and illumination configurations. The top 2 pictures illustrate the labradorescence of whichever twin appeared at the surface of a given patch on the (010) cleavage plane. In the right-hand pictures the back reflections from $(00\bar{1})$ are 6.9° apart, despite being sawcut at ~45°. Individual patches are partings on the perfect $(00\bar{1})$ cleavage and back reflecting. This is entirely a surface effect, in that a coating of an index matching fluid (mineral oil) completely removes the glow.

When cooled down to ambient temperatures, the high temperature forms will differentiate into two spatially separated feldspars. If the cooling is rapid (volcanism) the exchange of Alkalis, Na^+ and K^+, through the solid solution is somewhat inhibited, giving only small, but macroscopic, grains of the separated minerals (albite, microcline/orthoclase), forming perthite or antiperthite [Da Mommio-Plag]. Separation is much more difficult in the plageoclases, where Ca^{++} and Na^+ must be exchanged. Since these have differing charges, the Na needs to drag a Si to exchange with Ca and its accompanying Al. Although the cations Ca^{++} and Na^+ are small and can move relatively easily through the solid at high temperatures, the Si and Al are locked into tetrahedral sites, requiring special conditions to make them mobile. Figure 13 illustrates the relative scales for plageoclase vs. alkali unmixing under the same conditions.

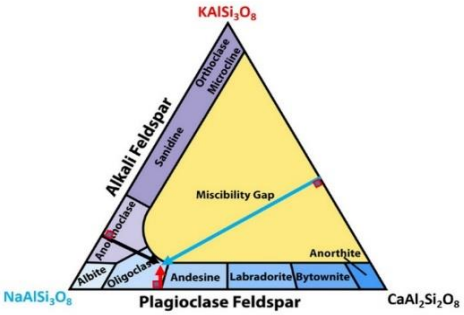

Figure 12.Feldspar Ternary Diagram [Da Mommio-Plag]. Single-phase feldspars can form continuous solid solutions of its 3 endmembers: anorthite, albite, and orthoclase. An equilateral triangle has the useful property that if you drop perpendiculars from any interior point to the three sides, the sum of their lengths will be a constant. Thus, every point can represent a unique blend of the end members (example: albite/blue 65%, orthoclase/red 10%, anorthite/black 25%). Compositions in the yellow miscibility gap cannot form a single feldspar solid solution. All feldspars crystalize in the triclinic system except for sanidine and orthoclase. Microcline is the triclinic low-temperature form of K feldspar.

The feldspar unmixing diagrams are shown in Figure 14. For Na rich plagioclase, Peristerite Unmixing separates oligoclase from albite forming peristerite. Bøggild and/or, perhaps, Huttenlocher Unmixing forms labradorite. For the alkali feldspars, high water pressure suppresses the melting temperature enough to be in contact with the unmixing solvus curve (see Figure 15) [Da

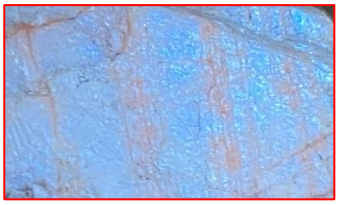

Figure 13 Blue peristerite labradorescence (125nm Na/Ca separation) is compared to red alkali antiperthite (4mm Na/K separation) a factor of 32,000. Canadian Beryllium mine E (AKA Beryl Pit). The uniformity of this sample also speaks to the quiescent environment during metamorphism.

thickness of the oligoclase, which would give ~π/2 phase between the 2 sets, making them largely independent and giving only a factor of 2 in the reflection.

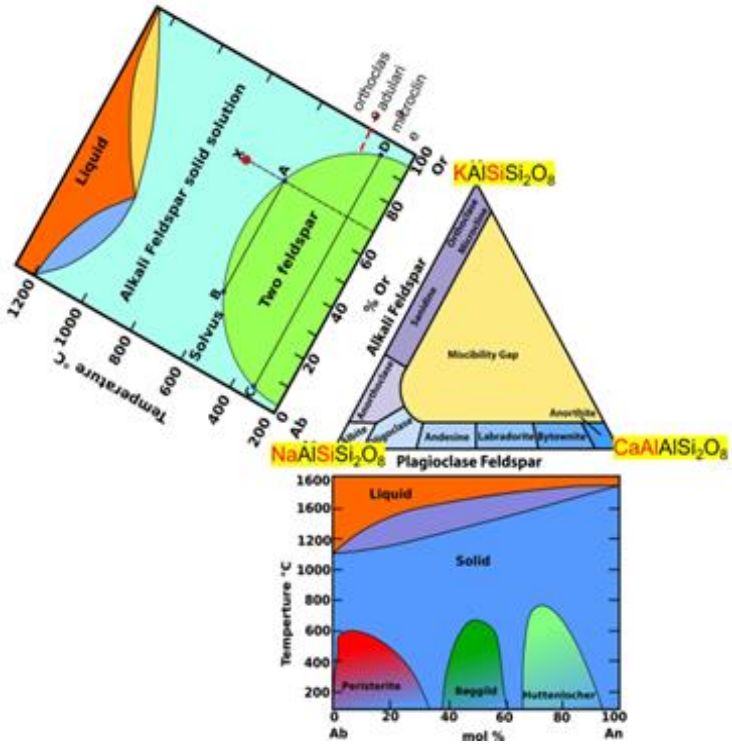

Figure 14. Unmixing Diagrams for Alkali and plagioclase feldspars. Crystallization as a single feldspar solid solution is stable at high temperature. However, at room temperature only the end members are truly stable.

The top left figure shows how unmixing occurs for the alkali feldspars [Da Mommio-Plag]. Take the example of composition X: 70% K,30% Na. As it cools down to the solvus curve at point A, a smaller portion of composition B segregates spatially. With further cooling the compositions follow the solvus curve B->C, A->D down to ambient temperature. Since Na^+ and K^+ are small and have the same charge, they can easily exchange through the solid when they are cooled slowly enough, forming macroscopic perthite. Very rapid cooling may only give microscopic separations.

Plagioclase unmixing (lower figure) [Da Mommio-Plag] is different: there are three solvus curves and the differing charges in the exchange of Ca^{++} with Na^+ requires exchanging CaAl with NaSi. The Al and Si occur in oxygenated tetrahedrons, which are large and much harder to diffuse through the solid.

Mommio-Plag]. In Figure 16, the alkali unmixing is extrapolated to higher water pressure and plagioclase unmixing is imagined such that agreement between alkali and plagioclse curves is achieved for albite (Ab). In their definitive paper (Figure 8) on peristerite structure, Fleet and Ribbe state "the presence of water under pressure at high temperatures permits the formation of occasional (OH) bonds at the tetrahedral vertices, thereby allowing the exchange of Al and Si from one tetrahedral site to another" [Ribbe 1964]. The imagined high water-pressure curve in Figure 16 need not have the liquid in contact with the solvus; from Figure 15, <10% anorthite peristerite composition should be liquid to below 700C and given long cooling times, optical scale unmixing is possible by diffusion through the solid solution.

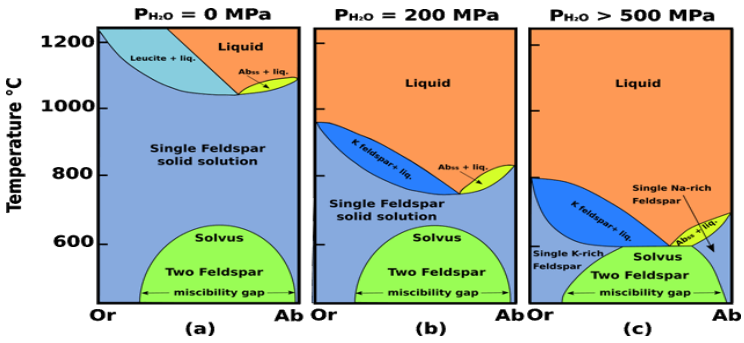

Figure 15 Alkali feldspar under high water pressure [Da Mommio-Plag]. By 500MPa=5kBar the melt is inContact with the solvus curve, allowing easy separation of the K-feldspar from the dominant albite to form anti-perthite.

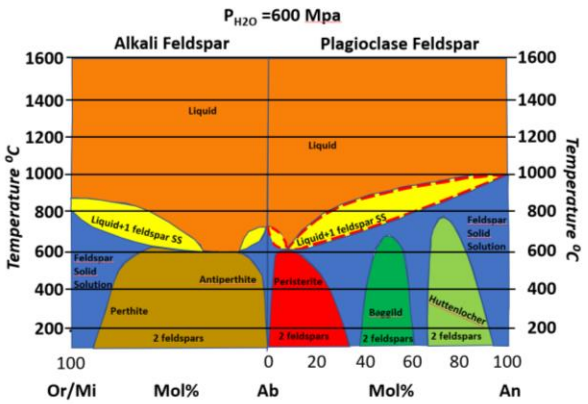

Figure 16. Extrapolating the alkali curves to 600MPa=6kBar and estimating the plagioclase curves to match the alkali composition for pure albite.

Geological setting

The Bancroft terrane is shown in Figure 17, along with the sources of fine optical peristerite (blue tags). The plum colored band is the CMBBZ (Central Metasedimentary Belt Boundary Zone) that separates the

Central Gneiss Belt to the northwest from the Central Metasedimentary Belt to the southeast, the latter is composed of several distinct terranes, each of which formed as an island archipelago off of the coast of what would be the supercontinent Rodinia (Figure 18). The Bancroft terrane is bordered (cyan line) by the Elzivir terrane to the southeast. In addition to the fine peristerites, the Bancroft terrane is home to a wide variety of rare minerals in its pegmatites, thus, the town of Bancroft styles itself as "the Mineral Capital of Canada".

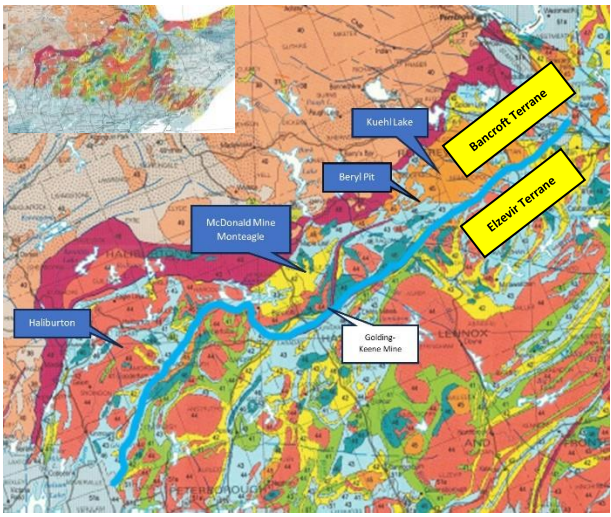

Figure 17. Overlay from [OntBedrock 2012] on Google Earth Pro, showing the island arc terranes stacked in the Central Metasedimentary Belt. Inset shows a wider view. Blue and white callouts locate the peristerite sources.

Specializing to the Beryl Pit (AKA Canadian Beryllium Mine E, and AquaRose E) [Berylpit mindat], [Rochefort 2015], it is assumed that the geologic thermal history was much the same for the other pegmatites (except for possible composition differences). The original beryl pegmatite was formed 1.28 BYA, when NYF (niobium-yttrium-fluorine) magma from a subducting plate rose into the over-riding crust as part of an island archipelago. It reached a plug at a depth of 20 to 30 km [Rochefort 2015] and solidified into huge crystals (Figure 19). The crystals are thought to have formed in as little as a year, due to the high pressure of H_20 (7kBar at those depths), despite the rapid initial cooling from intrusion into the country rock. The pegmatite seems to be very poor in calcium content, with only minor minerals apatite, euxenite, and fluorite having Ca in their stoichiometry. The bulk of the Ca is the small percentage found in the large amount of peristerite. While some separation of oligoclase from albite may have taken place during the formation episode, it is likely that they would be re-homogenized during the high-temperature phases of the later Grenville episode (see [Ribbe 1964]).

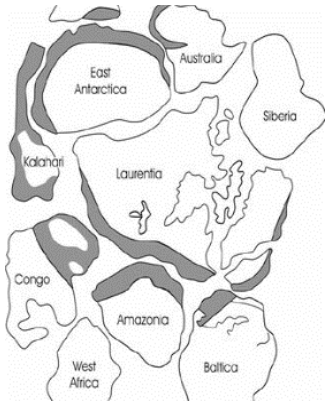

Figure 18. Hoffman's reconstruction of Rodinia [Behrmann 2007], showing the Grenville orogenic belts.

The Grenville Orogeny [Grenville-wikipedia 2023] involved the Central Gneiss Belt and successive terranes overriding the Superior Craton and each other, building, what some term, as the highest mountain range that has ever existed on earth (Figure 20). The main regonal- and contact-metamorphism took place in tne Bancroft terrane between 1045MYA and 1030MYA [Mezger 1992]. During this period, Figure 21 (from [van der Pluijm 2006]) displays the depth of the rocks that are currently at the surface. The red diamond shape represents the span of the Bancroft Terrane at a depth of 22 km, corresponding to 6 kbar [GeoPressures] of pressure (it may have still been saturated with H_2O). Once the temperature profile has equilibrated it should be about 600 C [wikiThermal 2023] at that depth. The cooling rate for all of the Grenville (presumably due to unloading from erosion of the mountains above) has been estimated as 2-4 ^oC/My [van der Pluijm 2006], giving ample quiescent cooling time through the peristerite solvus curve. Thus, the peristerite exosolution conditions in Figure 16 should have been present.

Figure 19. Large microcline/amazonite crystal from the beryl pit pegmatite. Described in [ODM 1953] as microcline micro-perthite. The green microcline (amazonite), still in the interior of the crystal, is thought to have been replaced on the surface and in cracks by red microcline.

The labradorescence is fairly consistent throughout the beryl pit pegmatite, despite forming in different layers in the initial island arc implacement. The large, creamy-white blocks in Figure 22 and Figure 2 were collected in the 1960s from one of two mounds (3-4 m high) containing almost no “interesting” mineralization from the ore body (ore was segregated in a 180 ton high-graded ore dump [ODM 1953]). These white blocks had been removed from the top portion of the pegmatite to get at the ore below. These peristerites show albite twinning at the 1-3 mm level and colored labradorescence throughout.

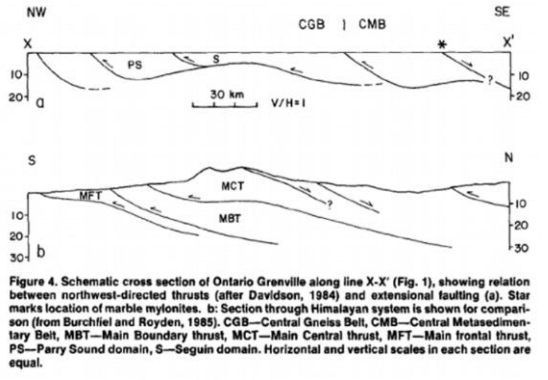

Figure 4. Schematic cross section of Ontario Grenville along line X-X' (Fig. 1), showing relation between northwest-directed thrusts (after Davidson, 1984) and extensional faulting (a). Star marks location of marble mylonites. b: Section through Himalayan system is shown for comparison (from Burchfiel and Royden, 1985). CGB—Central Gneiss Belt, CMB—Central Metasedimentary Belt, MBT—Main Boundary thrust, MCT—Main Central thrust, MFT—Main frontal thrust, PS—Parry Sound domain, S—Seguin domain. Horizontal and vertical scales in each section are equal.

Figure 20 Comparison of the Grenville terrane thrusting to that of the Himalayas [van der Pluijm 1989].

By 1990 a previous owner, upset with depradations on the ore dump, had the mounds and ore dump re-mixed. In 2018 the sample in Figure 23, containing some dark minerals (biotite and euxenite – radiation halos), was collected from the mix. The peristerite cabochon from that piece, Figure 24, is untwinned and more transparent than that from the creamy-white blocks. Finally, peristerite that is redder and finely twinned (0.1 - 0.3 mm), Figure 25, can be found in the pit floor now.

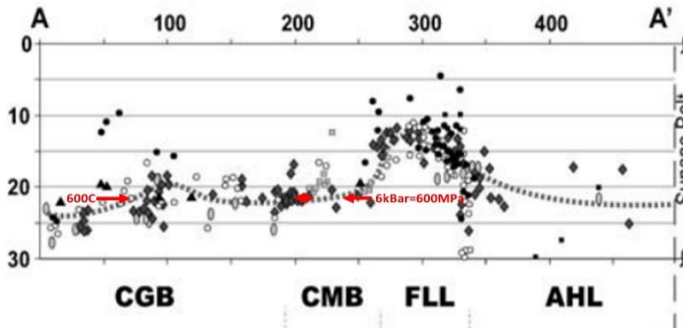

Figure 21 Depth of the present surface at 1000MYA [van der Pluijm 2006]. The red diamond indicates the position of the Bancroft Terrane (depth~22km) with pressure ~6kbar [GeoPressures]and temperature [wikiThermal 2023] ~600 °C.

The labradorescence of all these peristerites is essentially the same, no matter the melt chemistry, temperature history, or water pressure in the the various zones in the original pegmatite emplacement. Thus, the regional metamorphism seems to be crucial for the colorful displays.

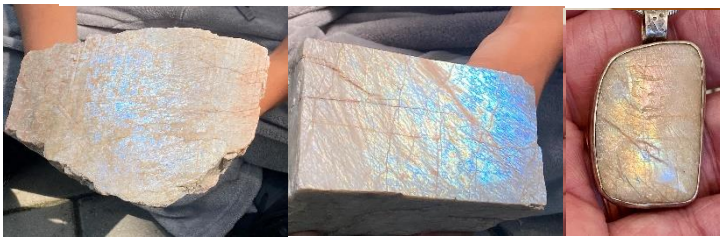
Figure 22. Creamy-white peristerite (collected 1960s) from the top of the pegmatite. Left: raw block as it came from the mound, (010) cleavage; middle: block sawn on (010); right:cabachon pendent cut from the middle block.

Conclusions

The structures and mechanisms for producing colorful labradorescence in peristerite are well understood as multi-layer dielectric (Bragg) mirrors, oriented in (0$\bar{8}$1) planes. The Bancroft samples were plausibly created in two episodes of mountain building: first, from a plugged, low-calcium alkalic pegmatite in an island archipellago, and second from regional metamorphism at the base of


Figure 23. peristerite from mixed ore and pegmatite cap regions of the Beryl Pit.


Figure 24 Cabochon cut from sample in Figure 23. Inset shows the finished pin.


Figure 25 Peristerite from the ore pit.

the Grenville orogeny. The slow cooling rate through the peristerite solvus allowed the unmixing to occur quiescently, resulting in very uniform structures. It is unknown what makes the Bancroft Terrane unique in its richness in rare minerals and half- to whole-wave spacing in its peristerites. Peristerites from other locations tend to labradorescence mainly blue, likely due to the difficulty in separating the Ca from the Na. The adularescent peristerite from Golding-Keene originated from near the Bancoft/Elziver boundary, which suffered a major decompression event [van der Pluijm 1989] during the Grenville. This could have added higher-pressure water, as compared to the other locations, which are found in the heart of the Bancroft Terrane. Possibly this resulted in thicker bilayers (>1.5 waves) and silvery-white reflections. As the names imply, labradorescence and adularescence are not confined to peristerites. The appendix summarizes Bøggild's careful work on orienting all the feldspar labradorizations.

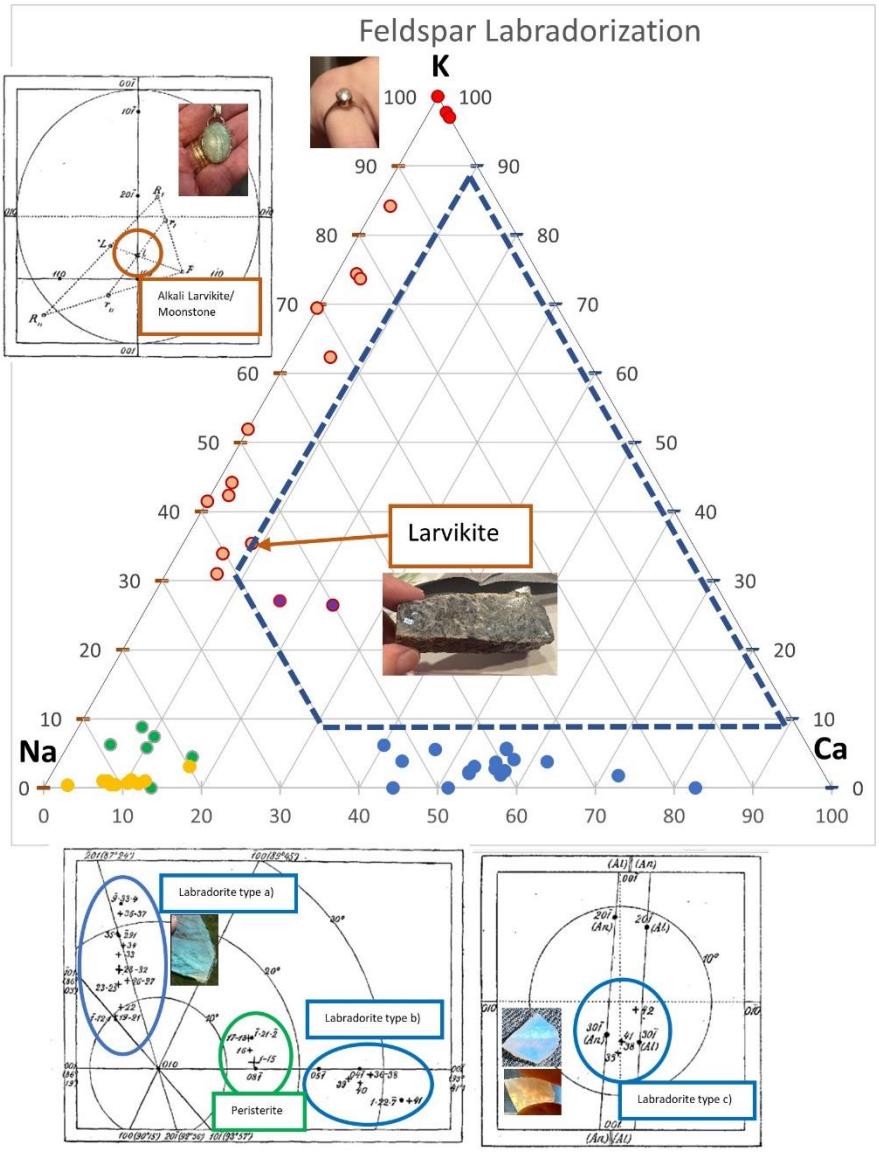

Figure 26 Summary of Bøggild's results. The central figure is the feldspar ternary diagram with orange, red, green, and blue dots representing Bøggild's composition data for orthoclase, adularia, peristerite, and labradorite, respectively. Yellow dots are Ribbe's peristerite composition data. The upper left diagram shows Bøggild's methodology for orienting the orthoclases. The orientations were quite consistent varying between 72° and 75° from the (001) direction. The lower left diagram shows Bøggild's orientations for his peristerite and labradorite types a) and b). Lower right shows labradorite type c). Top photo is an heirloom moonstone ring (presumably adularia). Photo in the orthoclase orientation diagram is a mixed amazonite/microcline cabochon from the beryl pit, showing adularescence. Photo lower left is a Madagascar type a) labradorite. Central photo shows a cm-grained larvikite. Lower right photos were of a slice cut from a ***transparent*** *moonstone from India. After its orientation was determined, it matched that of a type c) labradorite instead. The upper photo shows the bright blue and green reflections, while the lower photo shows the complementary colors in transmission.*

Appendix

Bøggild [Bøggild 1924] made a careful survey of labradorizations in the feldspars in samples from around the world. He concentrated on orienting the crystal directions that gave the colorful displays (Figure 26). Bøggild divided the feldspars into three groups: Orthoclase, Peristerites, and Labradorites. He looked principally at orientation but provided composition data where available from other sources or estimating from polarization properties. The orthoclase compositions are plotted in Figure 26 as red-rimmed orange dots (also red dots presumed to be adularia or purple dots composition errors). The orange dots are presumed to be

albite K-spar micro/nano-perthites, ranging from larvikite on the sodic end to moonstones near the potassic end. The green dots are Bøggild's peristerite data and the yellow dots are Ribbe's peristerite data. Bøggild's labradorites are shown as blue dots. Bøggild's orientations are shown in the angle-plots in Figure 26 and explained in the caption. The labradorites have three different orientations, sometimes exhibiting two different ones in the same sample. Further work on labradorite was done by [Jin 2021], who found a clear composition correlation with orientation in Bøggild's type a) labradorites. Pictures of some samples are included in association with orientation groups. The most recent plagioclase phase diagram is shown in Figure 27.

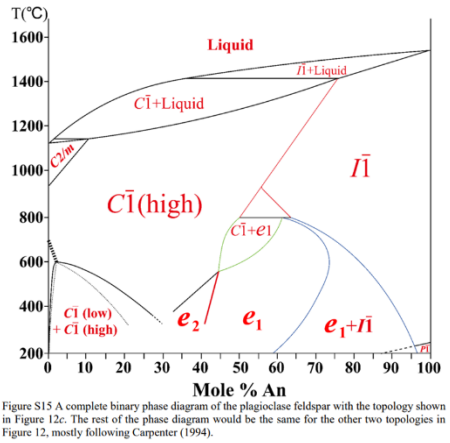

Figure S15 A complete binary phase diagram of the plagioclase feldspar with the topology shown in Figure 12*c*. The rest of the phase diagram would be the same for the other two topologies in Figure 12, mostly following Carpenter (1994).

Figure 27 Plagioclase phase diagram from [Jin 2021] supplemental information.

References

1. [Behrmann 2007] Behrmann J.H. et al., *Convergent Plate Boundaries and Collision Zones*, DOI:10.1007/978-3-540-68778-8_8, Figure 10, (PDF) Convergent Plate Boundaries and Collision Zones (researchgate.net)
2. [Berylpit mindat] mindat, Beryl Pit, Lyndoch Township, Brudenell, Lyndoch and Raglan, Renfrew County, Ontario, Canada (mindat.org)
3. [Bøggild 1924] Bøggild, O.B., On the Labradorization of the Feldspars. 1924. Available online: **http://gymarkiv.sdu.dk/MFM/kdvs/mfm%201-9/mfm-6-3.pdf** (accessed on 2 July 2021).
4. [Da Mommio-Plag] Da Mommio A. (ALEX STREKEISEN) webpage: ALEX STREKEISEN-Plagioclase-
5. [Fresnel] Fresnel equations - Wikipedia
6. [Geffcken 1939] Geffcken W., reference in Wikipedia-mirror, from H. Pulker, H.K. Pulker (1999): *Coatings on Glass,* Mirror - Wikipedia
7. [CN Dump 2023] CN Dump from Golding-Keene Quarry CN Rock Dump (CN Dump), Town of Bancroft, Hastings County, Ontario, Canada (mindat.org) webpage accessed Aug. 22, 2023.
8. [GeoPressures] GeoPressures.pdf (smith.edu)
9. [Goldsmith 1982] Goldsmith J.R., *Plagioclase stability at elevated temperatures and water pressures* American Mineralogist, Volume 67, pages 653-675, 1982. am67_653.pdf (minsocam.org)
10. [Grammatikopoulos 2005] Grammatikopoulos T.A. et al., *Genesis of the Olden wollastonite skarn, Sharbot Lake domain, Central Metasedimentary Belt, Grenville Province, southeastern Ontario, Canada*, Can. J. Earth Sci. Vol. 42, 2005, (PDF) Genesis of the Olden wollastonite skarn, Sharbot Lake domain, Central Metasedimentary Belt, Grenville Province, southeastern Ontario, Canada (researchgate.net).
11. [IGS 2023] International Gem Society, webpage What is Moonstone Gemstone? Value, Price, and Color - Gem Society accessed 22 August, 2023.
12. [Grenville-wikipedia 2023] Wikipedia viewed Aug. 17, 2023, Grenville orogeny - Wikipedia
13. [Jin 2021] Jin S., Xu H., and Lee S., *Revisiting the Bøggild Intergrowth in Iridescent Labradorite Feldspars: Ordering, Kinetics, and Phase Equilibria*, Minerals 2021, 11(7), 727,Figure 2, Minerals | Free Full-Text | Revisiting the Bøggild Intergrowth in Iridescent Labradorite Feldspars: Ordering, Kinetics, and Phase Equilibria (mdpi.com)

14. [Mezger 1992] Mezger K. et al., Contrib Mineral Petrol (1993) 114:13-26, *U-Pb geochronology of the Grenville Orogen of Ontario and New York: constraints on ancient crustal tectonics*, Contrib Mineral Petrol (1993) 114:15, U-Pb geochronology of the Grenville Orogen of Ontario and New York: constraints on ancient crustal tectonics (umich.edu)
15. [MindatPeri] Peristerite: Mineral information, data and localities. (mindat.org)
16. [moonstone MINDAT] Moonstone: Mineral information, data and localities. (mindat.org)
17. [Moreau 2020] Moreau A., et al*., Evolutionary algorithms converge towards evolved biological photonic structures*, Scientific Reports, Nature Research 2020 10:12023. https://doi.org/10.1038/s41598-020-68719-3
18. [ODM 1953] D. F. Hewitt, 62nd Annual Report Ont. Dept. Mines, *Geology of the Brudenell-Raglan Area*, Vol. LXII, part 5, pp. 36-42, 1953
19. [OntBedrock 2012] Ontario Ministry of Mines, *Bedrock geology of Ontario*, KML overlay for Google Earth Pro, 1:250 000 scale bedrock geology of Ontario - Dataset - Ontario Data Catalogue
20. [Ribbe 1964] RIBBE P.H,, FLEET S.G. *An electron-microscope study of peristerite plagioclases*. 1964. Available online: M35269017.TIF (rruff.info) (Accessed Aug. 17 2023).
21. [Rochefort 2015] Rochefort C. and Rai S.M. Mineralogy Group, Ottawa Lapsmith & Mineral Club, *Mineral Collecting Guide Beryl Pit*, Quadeville, Ont. 2015, Collecting Guide Beryl Pit.pdf (olmc.ca)
22. [Trap/Trail MINDAT] Trappers Trail peristerite occurrence, Dudley Township, Dysart et al, Haliburton County, Ontario, Canada (mindat.org) .
23. [Twinning] Crystal twinning - Wikipedia
24. [van der Pluijm 1989] van der Pluijm B. and Carlson K.A., *Extension in the Central Metasedimentary Belt of the Ontario Grenville: Timing and tectonic significance,* Geology 17(2), p. 163, 1989, (PDF) Extension in the Central Metasedimentary Belt of the Ontario Grenville: Timing and tectonic significance (researchgate.net)
25. [van der Pluijm 2006] van der Pluijm B. et al., *Restored transect across the exhumed Grenville orogen of Laurentia and Amazonia, with implications for crustal architecture,* Geology 34(8):p671 2006. DOI:10.1130/G22534.1, (PDF) Restored transect across the exhumed Grenville orogen of Laurentia and Amazonia, with implications for crustal architecture (researchgate.net)
26. [webmineral 2023] webmineral, Index of /data (webmineral.com).
27. [wikiThermal 2023] Wikipedia page on *Thermal Gradient in Earth's crust*. Geothermal gradient - Wikipedia